

# Exact solution for the two-site correlated Kondo-Lattice Model - a limiting case for a metal

T. Hickel,\* J. Röseler, and W. Nolting  
Lehrstuhl für Festkörpertheorie, Institut für Physik,  
Humboldt-Universität, 10115 Berlin  
(Dated: February 1, 2008)

The correlated Kondo-lattice model is used to describe the interaction of electrons in a single conduction band with localized magnetic moments as well as their mutual repulsion. It is our intention to provide an analytical exact result for this model by considering a two-site cluster. An equation-of-motion approach as well as the spectral theorem is chosen to obtain the complete expression for the one-particle Green's function. In a forgoing article the problem has been solved for an insulator, the present paper is devoted to the technical more demanding task of a metal.

## I. INTRODUCTION

The magnetism of a large variety of so-called local moment systems, like manganites, gadolinium or europium-chalcogenides, is governed by an interplay of the properties of magnetic moments localized at certain atoms and itinerant conduction electrons propagating through the lattice. If the system of localized spins  $\mathbf{S}_i$  were treated independently, a certain magnetic order could be explained with the help of a Heisenberg-like exchange coupling

$$\mathcal{H}_{ff} = - \sum_{i,j} J_{ij} \mathbf{S}_i \cdot \mathbf{S}_j. \quad (1)$$

In contrast to that the Kondo-lattice model tries to explain magnetic order via an indirect coupling of  $\mathbf{S}_i$  and  $\mathbf{S}_j$  mediated by the spin  $\sigma$  of the itinerant conduction electrons. The importance of the on-site interaction

$$\mathcal{H}_{sf} = - \frac{J}{\hbar} \sum_i \boldsymbol{\sigma}_i \cdot \mathbf{S}_i \quad (2)$$

was first emphasized by Zener<sup>1</sup>.

As far as the conduction electrons are concerned they might be described by their kinetic energy

$$\mathcal{H}_s = \sum_{i,j} \sum_{\sigma} T_{ij} c_{i\sigma}^{\dagger} c_{j\sigma}. \quad (3)$$

only. Here,  $c_{j\sigma}$  is a fermionic annihilation operator in second quantization. However, several authors<sup>2</sup> pointed out that at least for manganites with its relatively narrow  $e_g$ -bands an *ansatz* that neglects any electron-electron interaction is an insufficient treatment. This is because  $U$  is probably the largest energy scale in the problem.

Another indication of this insufficiency is the exact solution of the zero-bandwidth limit ( $T_{ij} = T_0 \delta_{ij}$ , also called *atomic limit*) of the Kondo-lattice model  $\mathcal{H}_s + \mathcal{H}_{sf}$ . In this limit the one-particle Green's function has an excitation spectrum of four energy poles<sup>3</sup>

$$\begin{aligned} \varepsilon_1 &= T_0 - \frac{\hbar}{2} JS, & \varepsilon_2 &= T_0 + \frac{\hbar}{2} J(S+1), \\ \varepsilon_3 &= T_0 - \frac{\hbar}{2} J(S+1), & \varepsilon_4 &= T_0 + \frac{\hbar}{2} JS, \end{aligned} \quad (4)$$

where  $S$  is defined by  $\mathbf{S}_i^2 = \hbar^2 S(S+1)$ . If the “test” electron enters an empty lattice site the energies  $\varepsilon_1$  or  $\varepsilon_2$  are necessary. The other two energies occur if the entered lattice site is already occupied. Apparently  $\varepsilon_3$  has the lowest energy for  $J > 0$ . Because of the involved Coulomb repulsion this is not understandable.

The simplest way to include electron-electron interaction in the Hamiltonian is an on-site Hubbard interaction

$$\mathcal{H}_{ss} = \frac{U}{2} \sum_i \sum_{\sigma} \hat{n}_{i\sigma} \hat{n}_{i-\sigma} = U \sum_i \hat{n}_{i\uparrow} \hat{n}_{i\downarrow}. \quad (5)$$

It has been shown<sup>2</sup> that this has an significant effect on the spectral function of the Kondo-lattice model. For the *atomic limit* calculation it implies that the energies  $\varepsilon_3$  and  $\varepsilon_4$  are shifted by  $U$  and  $\varepsilon_1$  becomes lowest.

The combination of all these possible effects in one Hamiltonian

$$\mathcal{H} = \mathcal{H}_s + \mathcal{H}_{ss} + \mathcal{H}_{sf} + \mathcal{H}_{ff}, \quad (6)$$

is in this paper called **correlated Kondo lattice model** (CKLM). Due to the fact that there is no analytical solution of the CKLM available, it is essential to obtain exact statements from limiting cases.

In a foregoing article<sup>4</sup> we explained, why especially the generalization of the *atomic limit* result to a two-site cluster is important for a better understanding of the CKLM. There, we investigated the Hamiltonian  $\mathcal{H}_s + \mathcal{H}_{sf}$  with an assumed hopping integral of the form

$$T_{ij} = \begin{cases} \tilde{T} & i \neq j \text{ and } i, j \text{ in same cluster,} \\ T_0 & i = j, \\ 0 & i, j \text{ in different clusters.} \end{cases}$$

The part  $\mathcal{H}_{ff}$  was omitted to gain the chance for a connection of the cluster to the lattice. This is possible if expectation values of spin operators, like  $\langle S_1^z \rangle$  are not uniquely determined by the properties of the cluster. Furthermore, a Hamiltonian without  $\mathcal{H}_{ff}$  is much easier to handle. The part  $\mathcal{H}_{ss}$ , on the other hand, was redundant since the limit of an empty conduction band was considered. For this situation, which is related to an insulator, we were able to give the complete analytical expression for the one-particle Green's function as obtained by a solution of the equations of motion.

With the present paper we try to obtain similar results for metals. Since the occupation of the conduction band is now arbitrary, the mathematical systems that need to be solved are about one order of magnitude larger than in the case of an insulator. Additionally, it is necessary to take the Hubbard interaction into account. Therefore, we consider the Hamiltonian

$$\begin{aligned} \bar{\mathcal{H}} = & \tilde{T} \sum_{\sigma=\uparrow,\downarrow} \left( c_{1\sigma}^\dagger c_{2\sigma} + c_{2\sigma}^\dagger c_{1\sigma} \right) + \sum_{\alpha=1}^2 \sum_{\sigma=\uparrow,\downarrow} \frac{U}{2} \hat{n}_{\alpha\sigma} \hat{n}_{\alpha-\sigma} \\ & + \sum_{\alpha=1}^2 \sum_{\sigma=\uparrow,\downarrow} \left\{ T_0 \hat{n}_{\alpha\sigma} - \frac{J}{2} \left( z_\sigma S_\alpha^z \hat{n}_{\alpha\sigma} + S_\alpha^\sigma c_{\alpha-\sigma}^\dagger c_{\alpha\sigma} \right) \right\}, \end{aligned} \quad (7)$$

where  $S^\uparrow \equiv S^+$ ,  $S^\downarrow \equiv S^-$  and  $z_\uparrow \equiv +1$ ,  $z_\downarrow \equiv -1$ . For simplicity we restrict ourself to  $S = 1/2$ .

Despite of the larger effort, we use the same techniques already proposed for the insulator. What has been explained on the more concise problem there, can now be applied directly. It will not be possible to provide every detail of the calculations here. A thorough documentation of all necessary transformations can be found elsewhere<sup>5</sup>.

## II. SOLUTION FOR THE EQUATIONS OF MOTION

To describe the properties of the electronic partial system of the cluster we are especially interested in the one-electron retarded Green's function  $\langle\langle c_{i\sigma}; c_{j\sigma}^\dagger \rangle\rangle_E$ . This function is closely related to the spectral density and contains all information about possible single-particle excitations.

The method of choice is an equation-of-motion technique. Compared to a direct determination of the Lehmann representation it has two advantages. First, an equation of motion

$$E \langle\langle \hat{A}; \hat{B} \rangle\rangle_E = \hbar \langle [\hat{A}, \hat{B}]_+ \rangle + \langle\langle [\hat{A}, \bar{\mathcal{H}}]_-; \hat{B} \rangle\rangle_E. \quad (8)$$

contains as an inhomogeneity a correlation function  $\langle [\hat{A}, \hat{B}]_+ \rangle$ . This will directly appear in the numerator of the Green's function, without being forced to actually calculate the expectation value. Therefore, we are able to discuss the dependence of the spectral weights on parameters as the averaged band occupation or the averaged  $z$ -component of the localized spins. Secondly, each equation of motion contains higher Green's functions  $\langle\langle [\hat{A}, \bar{\mathcal{H}}]_-; \hat{B} \rangle\rangle_E$ . Hence, by using intelligent techniques we do not only get  $\langle\langle \hat{A}; \hat{B} \rangle\rangle_E$  but a complete set of Green's function with much more information. We will make use of this fact in the next section.

Since we are dealing with a finite size system, the hierarchy of equations of motion necessarily has to terminate. The complete set of 1040 equations can be formulated as a single matrix equation. By unitary transformations

this matrix needs to be reduced to blocks of a size which can be solved directly. A first step in this direction is the implementation of the site symmetry. Therefore, we define combined Green's functions

$$\begin{aligned} \langle\langle \hat{C}_s \hat{D}_{\bar{s}} c_{s\sigma} \rangle\rangle^{(\epsilon)} = & \langle\langle \hat{C}_s \hat{D}_{\bar{s}} c_{s\sigma}; c_{s\sigma}^\dagger \rangle\rangle_E \\ & + \epsilon \langle\langle \hat{C}_{\bar{s}} \hat{D}_s c_{\bar{s}\sigma}; c_{s\sigma}^\dagger \rangle\rangle_E, \end{aligned} \quad (9)$$

where the site index  $\bar{s}$  represents the opposite of site  $s$  ( $s = 1 \Rightarrow \bar{s} = 2$ ;  $s = 2 \Rightarrow \bar{s} = 1$ ),  $\hat{C}_s$  and  $\hat{D}_{\bar{s}}$  are arbitrary products of spin- and Fermi-operators. The two partial systems for  $\epsilon = +1$  and  $\epsilon = -1$  can be solved separately and simultaneously (they only differ in the sign of  $\tilde{T}$ ).

Even if additionally the mirror symmetry with respect to the spin quantization axis is used, one is still left with the large number of Green's function listed below:

$$\begin{aligned} G_A^{(\epsilon)} &= \langle\langle \hat{S} c_{s\sigma} \rangle\rangle^{(\epsilon)} & K_A^{(\epsilon)} &= \langle \hat{S} \rangle \\ G_B^{(\epsilon)} &= \langle\langle \hat{S} \hat{n}_{s-\sigma} c_{s\sigma} \rangle\rangle^{(\epsilon)} & K_B^{(\epsilon)} &= \langle \hat{S} \hat{n}_{s-\sigma} \rangle \\ G_C^{(\epsilon)} &= \langle\langle \hat{S} \hat{n}_{\bar{s}-\sigma} c_{s\sigma} \rangle\rangle^{(\epsilon)} & K_C^{(\epsilon)} &= \langle \hat{S} \hat{n}_{\bar{s}-\sigma} \rangle \\ G_D^{(\epsilon)} &= \epsilon \langle\langle \hat{S} c_{s-\sigma}^\dagger c_{\bar{s}-\sigma} c_{s\sigma} \rangle\rangle^{(\epsilon)} & K_D^{(\epsilon)} &= \epsilon \langle \hat{S} c_{s-\sigma}^\dagger c_{\bar{s}-\sigma} c_{s\sigma} \rangle \\ G_E^{(\epsilon)} &= \epsilon \langle\langle \hat{S} c_{\bar{s}-\sigma}^\dagger c_{s-\sigma} c_{s\sigma} \rangle\rangle^{(\epsilon)} & K_E^{(\epsilon)} &= \epsilon \langle \hat{S} c_{\bar{s}-\sigma}^\dagger c_{s-\sigma} c_{s\sigma} \rangle \\ G_F^{(\epsilon)} &= \langle\langle \hat{S} \hat{n}_{\bar{s}\sigma} c_{s\sigma} \rangle\rangle^{(\epsilon)} & K_F^{(\epsilon)} &= \langle \hat{S} \hat{n}_{\bar{s}\sigma} \rangle \\ G_G^{(\epsilon)} &= \langle\langle \hat{S} \hat{n}_{\bar{s}-\sigma} \hat{n}_{s-\sigma} c_{s\sigma} \rangle\rangle^{(\epsilon)} & K_G^{(\epsilon)} &= \langle \hat{S} \hat{n}_{\bar{s}-\sigma} \hat{n}_{s-\sigma} \rangle \\ G_H^{(\epsilon)} &= \epsilon \langle\langle \hat{S} \hat{n}_{\bar{s}\sigma} c_{s-\sigma}^\dagger c_{\bar{s}-\sigma} c_{s\sigma} \rangle\rangle^{(\epsilon)} & K_H^{(\epsilon)} &= \epsilon \langle \hat{S} \hat{n}_{\bar{s}\sigma} c_{s-\sigma}^\dagger c_{\bar{s}-\sigma} c_{s\sigma} \rangle \\ G_I^{(\epsilon)} &= \epsilon \langle\langle \hat{S} \hat{n}_{\bar{s}\sigma} c_{\bar{s}-\sigma}^\dagger c_{s-\sigma} c_{s\sigma} \rangle\rangle^{(\epsilon)} & K_J^{(\epsilon)} &= \epsilon \langle \hat{S} \hat{n}_{\bar{s}\sigma} c_{\bar{s}-\sigma}^\dagger c_{s-\sigma} c_{s\sigma} \rangle \\ G_K^{(\epsilon)} &= \langle\langle \hat{S} \hat{n}_{\bar{s}\sigma} \hat{n}_{s-\sigma} c_{s\sigma} \rangle\rangle^{(\epsilon)} & K_K^{(\epsilon)} &= \langle \hat{S} \hat{n}_{\bar{s}\sigma} \hat{n}_{s-\sigma} \rangle \\ G_L^{(\epsilon)} &= \langle\langle \hat{S} \hat{n}_{\bar{s}\sigma} \hat{n}_{\bar{s}-\sigma} c_{s\sigma} \rangle\rangle^{(\epsilon)} & K_L^{(\epsilon)} &= \langle \hat{S} \hat{n}_{\bar{s}\sigma} \hat{n}_{\bar{s}-\sigma} \rangle \\ G_M^{(\epsilon)} &= \langle\langle \hat{S} \hat{n}_{\bar{s}-\sigma} \hat{n}_{\bar{s}\sigma} \hat{n}_{s-\sigma} c_{s\sigma} \rangle\rangle^{(\epsilon)} & K_M^{(\epsilon)} &= \langle \hat{S} \hat{n}_{\bar{s}-\sigma} \hat{n}_{\bar{s}\sigma} \hat{n}_{s-\sigma} \rangle \end{aligned}$$

Here,  $\hat{S}$  stands for all possible products of spin operators. If, as assumed,  $S = 1/2$  there are 10 such possibilities. The right column gives for each Green's function the corresponding correlation function emerging in its equation of motion. It is useful to group these functions into four *density classes*, determined by the number of fermionic creation operators in its active part:

$$\begin{aligned} G_I &: G_A, \\ G_{II} &: G_B, G_C, G_D, G_F, G_R, \\ G_{III} &: G_G, G_H, G_J, G_K, G_L, \\ G_{IV} &: G_M. \end{aligned}$$

The Green's functions of density class IV vanish whenever the number of participating electrons is smaller than 3. The ones in density class III vanish if we have less than 2 electrons etc.. Using this notation the matrix equation

of all Green's functions has the block structure

$$\begin{pmatrix} \boxed{M_I} & M_{I,II} & 0 & 0 \\ 0 & \boxed{M_{II}} & M_{II,III} & 0 \\ 0 & 0 & \boxed{M_{III}} & M_{III,IV} \\ 0 & 0 & 0 & \boxed{M_{IV}} \end{pmatrix} \begin{pmatrix} G_I \\ \overline{G_{II}} \\ \overline{G_{III}} \\ \overline{G_{IV}} \end{pmatrix} = \begin{pmatrix} K_I \\ \overline{K_{II}} \\ \overline{K_{III}} \\ \overline{K_{IV}} \end{pmatrix}, \quad (10)$$

where the right hand side represents the column of all inhomogeneities appearing in every equation of motion.

Since the matrix has a triangular shape, the remaining task is to find the inverse of the blocks  $M_I$ ,  $M_{II}$ ,  $M_{III}$  and  $M_{IV}$ . It is therefore possible to stay in certain density classes, which justifies the grouping. Additionally, we can benefit from particle-hole symmetry. It implies that the density classes I and IV as well as the classes II and III can be treated in a similar way, respectively.

The density class I consists of the 10 Green's functions with only one fermionic operator but with several spin operators. If one could assume that all Green's functions of the other density classes vanish, one just had to invert the matrix  $M_I$  to get a solution. The assumption is fulfilled if and only if one describes an insulator with a single excess electron in a otherwise empty conduction band. The foregoing article<sup>4</sup> was devoted to these materials. In the case of arbitrary band occupations we have to solve the equation  $M_I \cdot G_I = K_I - M_{I,II} G_{II}$ . Since only the right hand side is modified we can use the same rules for the combination of spin operators in the Green's functions as in the case of an insulator to simplify  $M_I$ .

Matrix  $M_{II}$  is also simplified by an intelligent combination of Green's functions. As far as the spin operators are concerned we use again the rules proposed in the treatment of an insulator. To get an idea about the behavior of the fermionic operators we investigated another limiting case: If in  $\mathcal{H}$  the parameter  $J$  is set to 0 we have a system without any spin operator, namely a Hubbard cluster. Its solution is sketched in appendix A. The rules for a formation of combined Green's functions used there can then be applied to equation (10).

This technique to combine Green's functions by a successive treatment of the spin operators and the fermionic operators respectively works, but is rather lengthy and fault-prone. When doing this job we learned that a simple text editor can be awesomely helpful. Already when generating the 1040 equations of motion a **cut-and-paste** mechanism can be used effectively, since the same commutators  $[c_{s\sigma}, \mathcal{H}]_-$ ,  $[S_s^z, \mathcal{H}]_-$  and  $[S_s^\sigma, \mathcal{H}]_-$  have to be implemented several times. For combinations the **search-and-replace** function is quite helpful.

Appendix B gives detailed instructions which Green's functions need to be summed and subtracted to achieve a simpler structure of  $M_{II}$ . If implemented one obtains matrix blocks of size  $3 \times 3$ . There are four types of these matrices:

$$M_0^{(\mu_1 \mu_2 \mu_3 \mu_4)}(\hat{E}) = \begin{pmatrix} \hat{E} + 2\mu_4 a & \mu_1 \tilde{T} & 0 \\ \mu_1 \tilde{T} & \hat{E} & \mu_2 2a \\ 0 & \mu_2 2a & \hat{E} + \mu_3 \tilde{T} \end{pmatrix} \quad (11)$$

$$M_1^{(\mu_2 \mu_5)}(\hat{E}) = \begin{pmatrix} \hat{E} + \mu_5 U & 0 & 0 \\ 0 & \hat{E} & \mu_2 2a \\ 0 & \mu_2 2a & \hat{E} \end{pmatrix}, \quad (12)$$

$$M_2^{(\mu_1 \mu_2 \mu_5)}(\hat{E}) = \begin{pmatrix} \hat{E} + \mu_5 U & \mu_1 2\tilde{T} & 0 \\ \mu_1 2\tilde{T} & \hat{E} & \mu_2 2a \\ 0 & \mu_2 2a & \hat{E} \end{pmatrix}, \quad (13)$$

$$M_3^{(\mu_6)}(\hat{E}) = \begin{pmatrix} \hat{E} + \mu_6 U & 2\tilde{T} & 0 \\ 2\tilde{T} & \hat{E} & 6\mu_6 a \\ 0 & 2\mu_6 a & \hat{E} + 4\mu_6 a \end{pmatrix} \quad (14)$$

Here, we used the abbreviation  $a = \frac{\hbar}{2} \frac{J}{2}$  and  $\mu_1, \dots, \mu_6$  are sign parameters.  $M_0$ , which already played a role in the insulator problem<sup>4</sup>, has the eigenvalues

$$\begin{aligned} \hat{E}_{01}^{(\mu_3 \mu_4)} &= \mu_3 \tilde{T} + 2\mu_4 a, \\ \hat{E}_{02}^{(\mu_3 \mu_4)} &= -\sqrt{4a^2 - 2\mu_3 \mu_4 a \tilde{T} + \tilde{T}^2}, \\ \hat{E}_{03}^{(\mu_3 \mu_4)} &= +\sqrt{4a^2 - 2\mu_3 \mu_4 a \tilde{T} + \tilde{T}^2}. \end{aligned}$$

The other matrices are connected to non-vanishing electron-densities as can be seen at the appearance of  $U$ . The structure of  $M_1$  is simple, and its eigenvalues are

$$\hat{E}_{11}^{(\mu_5)} = \mu_5 U, \quad \hat{E}_{12} = 2a, \quad \hat{E}_{13} = -2a. \quad (15)$$

In contrast to that the determinantal polynomial of  $M_2$

$$0 \stackrel{!}{=} \hat{E}^3 + \mu_5 \hat{E}^2 U - 4\hat{E} (a^2 + \tilde{T}^2) - 4a^2 \mu_5 U \quad (16)$$

can only be factorized with Cardan's formulas. The three eigenvalues of this cubic equation are

$$\hat{E}_{21}^{(\mu_5)} = \mu_5 \frac{U}{3} - \frac{2}{3} \Re C_2, \quad (17)$$

$$\hat{E}_{22}^{(\mu_5)} = \mu_5 \frac{U}{3} + \frac{1}{3} [\Re C_2 + \sqrt{3} \Im C_2] \quad (18)$$

$$\text{and } \hat{E}_{23}^{(\mu_5)} = \mu_5 \frac{U}{3} + \frac{1}{3} [\Re C_2 - \sqrt{3} \Im C_2], \quad (19)$$

$$\text{where } C_2 = \sqrt[3]{\mu_5 A_2 + i \sqrt{B_2^3 - A_2^2}}$$

$$\text{and } A_2 = 36a^2 U - 18\tilde{T}^2 U - U^3$$

$$B_2 = 12a^2 + 12\tilde{T}^2 + U^2.$$

Similarly, we have for  $M_3$  the cubic equation

$$\begin{aligned} 0 \stackrel{!}{=} \hat{E}^3 + \mu_6 \hat{E}^2 (4a + U) - 4\hat{E} (3a^2 + \tilde{T}^2 - aU) \\ - \mu_6 4a (4\tilde{T}^2 + 3aU), \end{aligned} \quad (20)$$

with the three solutions

$$\hat{E}_{31}^{(\mu_6)} = \frac{\mu_6}{3} (U + 4a) - \frac{2}{3} \Re C_3, \quad (21)$$

$$\hat{E}_{32}^{(\mu_6)} = \frac{\mu_6}{3} (U + 4a) + \frac{1}{3} [\Re C_3 + \sqrt{3} \Im C_3] \quad (22)$$

$$\text{and } \hat{E}_{33}^{(\mu_6)} = \frac{\mu_6}{3} (U + 4a) + \frac{1}{3} [\Re C_3 - \sqrt{3} \Im C_3] \quad (23)$$

where  $C_3 = \sqrt[3]{\mu_6 A_3 + i\sqrt{B_3^3 - A_3^2}}$ ,

$$\begin{aligned} A_3 &= -280a^3 + 132a^2U - 18\tilde{T}^2U - U^3 + 6a(24\tilde{T}^2 + U^2) \\ B_3 &= 52a^2 + 12\tilde{T}^2 - 4aU + U^2. \end{aligned}$$

If the eigenvalue problem of the cluster is studied and especially the Hilbert subspace of two electrons in the conduction band is considered, one is confronted with exactly the same two cubic equations (16) and (20). This underlines the close relationship of the eigenvalue problem and the equation-of-motion technique.

To determine the inverse of  $M_x, x = 0, \dots, 3$  it is sufficient to know its eigenvectors. As explained more detailed in the treatment of the insulator<sup>4</sup>, basic algebra then immediately allows to give an expression for  $M_x^{-1}$ :

$$M_x^{-1}[ij] = \sum_{k=1}^3 \frac{m_{xk}(i, j)}{\hat{E} + \hat{E}_{xk}}, \quad (24)$$

with well defined coefficients  $m_{xk}(i, j)$ . This structure is particularly suitable because we intend to get the analytic expression for the one-particle Green's function as

$$G(E) = \langle\langle \hat{A}; \hat{B} \rangle\rangle_{E+i0^+} = \sum_{k=1}^p \frac{\hbar\alpha_k}{E - E_k + i0^+}, \quad (25)$$

with  $p$  linear energy poles. Since we succeeded to find combined Green's functions which are connected in  $3 \times 3$  systems, an inversion of the matrices like in (24) will ensure that every combined Green's function has the form (25). To return to the original Green's functions one just has to undo the combinations. That happens by summations and subtractions of the combined expressions and will therefore maintain the form (25).

We mentioned above that the calculations can be done within certain density classes. To be more precise, to solve equation (10) the following four matrix equations have to be considered:

$$\begin{aligned} \text{IV} : \quad & M_{\text{IV}} \cdot G_{\text{IV}} = K_{\text{IV}} \\ \text{III} : \quad & M_{\text{III}} \cdot G_{\text{III}} = K_{\text{III}} - M_{\text{III,IV}} G_{\text{IV}} \\ \text{II} : \quad & M_{\text{II}} \cdot G_{\text{II}} = K_{\text{II}} - M_{\text{II,III}} G_{\text{III}} \\ \text{I} : \quad & M_{\text{I}} \cdot G_{\text{I}} = K_{\text{I}} - M_{\text{I,II}} G_{\text{II}} \end{aligned} \quad (26)$$

One has to obey this order, because apart from system IV we always have an input of a class with higher electron densities. On the one hand, the matrix multiplication on the right side implies an additional summation of already calculated Green's functions. On the other hand, a partial fraction expansion is necessary to return to the form (25).

$$\begin{aligned} \frac{K_{\text{III}} - \frac{K_{\text{IV}}}{E - E_{\text{IV}}}}{E - E_{\text{III}}} &= \frac{K_{\text{III}}}{E - E_{\text{III}}} - \frac{K_{\text{IV}}}{(E - E_{\text{III}})(E - E_{\text{IV}})} \\ &= \frac{K_{\text{III}}}{E - E_{\text{III}}} + \frac{K_{\text{IV}}}{E_{\text{IV}} - E_{\text{III}}} \left( \frac{1}{E - E_{\text{III}}} - \frac{1}{E - E_{\text{IV}}} \right) \end{aligned} \quad (27)$$

Occasionally, it happens that  $E_{\text{III}} = E_{\text{IV}}$ , leading to quadratic energy poles. However, after performing all necessary summations the spectral weight of these poles will always vanish.

Taking all this into account, one obtains after a straightforward calculation expressions for the Green's functions of density class I. If furthermore all combinations are undone, the desired analytical exact result for the one-electron Green's function  $\langle\langle c_{s\sigma}; c_{s\sigma}^\dagger \rangle\rangle_E$  can be given. It consists of 102 energy poles.

Six of them, namely the energies

$$E = T_0 + a - \hat{E}_{0k}^{(++)} \quad \text{and} \quad (28)$$

$$E = T_0 + a - \hat{E}_{0k}^{(-+)} \quad \text{for } k = 1, 2, 3, \quad (29)$$

are a result of the inversion of  $M_{\text{I}}$ . They are just a subset of the energies

$$E = T_0 - a - \hat{E}_{1l}^{(-)} - \hat{E}_{0k}^{(\pm-)}, \quad (30)$$

$$E = T_0 - a - \hat{E}_{2l}^{(-)} - \hat{E}_{0k}^{(\pm-)} \quad \text{and} \quad (31)$$

$$E = T_0 - a - \hat{E}_{3l}^{(-)} - \hat{E}_{0k}^{(\pm-)} \quad \text{for } k, l = 1, 2, 3 \quad (32)$$

which occur, if  $M_{\text{II}}$  is inverted. The structure of these energy poles is quite clear. The Green's functions of density class II include excitation processes from a one-electron state to a two-electron state. The energies of the first are mediated by the eigenvalues of  $M_0$ , the energies of the latter are connected to the matrices  $M_1, M_2$  and  $M_3$ .  $T_0$  is just a trivial energy shift.  $-a$  actually belongs into the definition of  $M_0$ . The super-index " $\pm$ " in  $\hat{E}_{0k}$  illustrates that always both possible signs of  $\tilde{T}$  need to be considered, as mentioned subsequently to (9). Hence,  $M_{\text{II}}$  leads to  $3 \times 3 \times 3 \times 2 = 54$  energy poles.

It has already been pointed out, that  $M_{\text{III}}$  can be treated similarly to  $M_{\text{II}}$  according to the particle-hole symmetry of the system. This symmetry can be investigated more thoroughly when the Hamiltonian is reformulated in terms of hole-creation and -annihilation operators,  $b_{i-\sigma}^\dagger = z_\sigma c_{i\sigma}$ . It leads to the result that with an energy pole  $E_k = T_0 + f(\tilde{T}, J, U)$  of the one-particle Green's function,  $\bar{E}_k = U + T_0 - f(-\tilde{T}, J, U)$  is an energy pole, too. Applied to (30)- (32) one gets all the energies related to the matrices  $M_{\text{III}}$  and  $M_{\text{IV}}$ . Since

$$T_0 - a - \hat{E}_{11}^{(-)} - \hat{E}_{0k}^{(\pm-)} = T_0 + U + a + \hat{E}_{11}^{(-)} + \hat{E}_{0k'}^{(\mp-)}, \quad (33)$$

we have six degenerate energies, leading to  $p = 2 \times 54 - 6 = 102$  energy poles of the one-particle Green's function  $\langle\langle c_{i\sigma}; c_{i\sigma}^\dagger \rangle\rangle_E$  and all higher Green's functions.

All these excitation energies are functions of the model parameter  $\tilde{T}, U$  and  $J$ . Since the cluster is a generalization of the *atomic limit*, the  $\tilde{T}$ -dependence is of special interest (see figure 1). Because of the large number of energy lines, the formation of two Hubbard bands can clearly be seen. Although they are well separated at small  $\tilde{T}$ , there seems to be an overlap of the bands above 0.5 eV. When going to higher values of  $\tilde{T}$  a separation of

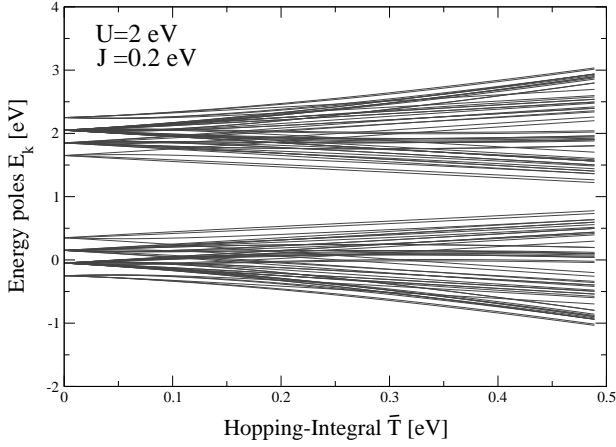


FIG. 1: Dependence of every energy poles of the one-particle Green's function on the hopping integral  $\tilde{T}$ . The fixed model parameters are:  $T_0 = 0$  eV,  $U = 2$  eV and  $J = 0.2$  eV.

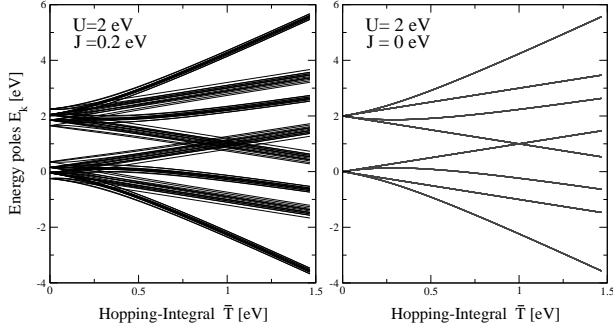


FIG. 2: Dependence of the energy poles on the hopping integral  $\tilde{T}$ . At the left the behaviour of the CKLM is shown, for comparison the Hubbard cluster ( $J = 0$ ) is investigated at the right for the same parameter range.

the bands and a formation of bundles occurs. As can be seen when the two parts of figure 2 are compared each of these bundles results from the  $J$ -splitting of an energy pole obtained for the two-site Hubbard cluster (appendix A). This splitting can best be shown, if, as in figure 3, the  $J$ -dependence of the energy poles is studied. The picture suggests a symmetry with respect to the sign of  $J$ , but this is not completely given.

Coming back to figure 1 another striking fact needs to be mentioned. It concerns the limit  $\tilde{T} \rightarrow 0$ , which is identically to the situation of the *atomic limit*. As noted in (4) we expect in this limit a reduction to four energy poles. In contrast to that we obtain twice as many energy lines for  $\tilde{T} = 0$  in figure 1. Obviously, the energies alone are insufficient to describe excitation processes. Remarks on the corresponding spectral weights are necessary.

The routine we suggested for the solution of the equations of motion inevitably gives for each Green's function these spectral weights, too. The fact that we don't give the complete analytical solution here, has two main reasons. First of all, the routine consists of quite a lot of

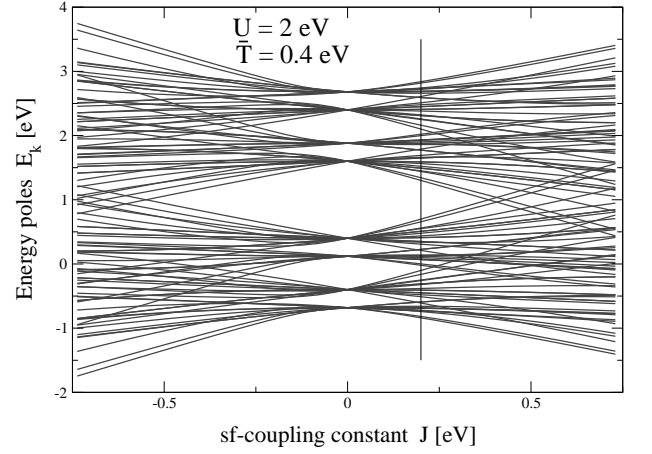


FIG. 3: Dependence of the energy poles on the sf-coupling constant  $J$ . The fixed model parameters are:  $T_0 = 0$  eV,  $U = 2$  eV and  $\tilde{T} = 0.4$  eV. The vertical line marks the  $J$  value of figure 1.

complicated summations: The combined Green's function for instance are just sums. At least one summation is necessary to get the inverse of a single matrix as given by equation (24). Their multiplication with a column of correlation functions as well as the matrix multiplications in each of the lines of (26) imply further sums. At the end partial fraction expansions have to be performed and the combinations of Green's functions needs to be undone. Even so, all this is simple arithmetics it leads to really lengthy expressions for the spectral weights. Secondly, the spectral weights of each Green's function depend in principle on all correlation functions that appear in inhomogeneities of the same or higher density classes. For  $\langle\langle c_{1\uparrow}; c_{1\uparrow}^\dagger \rangle\rangle_E$  this means a dependence on 1040 correlation functions ( $1/3$  is zero by definition). All of them need to be specified. Only afterwards the result for the spectral weights is really meaningful.

### III. TREATMENT OF THE CORRELATION FUNCTIONS

Already when dealing with the limiting case of an empty conduction band<sup>4</sup> one has to develop concepts for the determination of the emerging spin correlation functions. On the one hand, a simpler Hamiltonian, that describes the spin system and includes lattice effects like anisotropy or molecular fields, can be investigated. Alternatively, the spectral theorem provides information on these correlation functions. The latter concept implies that all calculations are based on the cluster Hamiltonian only and no connection to the lattice is made. In this paper we are going to use a combination of these two concepts.

As mentioned before, it is a crucial advantage of our methods that besides  $\langle\langle c_{i\sigma}; c_{i\sigma}^\dagger \rangle\rangle_E$  a complete set of all Green's functions participating in the equations of mo-

tion is obtained. For an arbitrary Green's function, by construction given in the form (25), the spectral theorem allows the calculation of a corresponding correlation function

$$\langle \hat{B}\hat{A} \rangle = \sum_{k=1}^p \alpha_k f_-(E_k) = \sum_{k=1}^p \frac{\alpha_k}{e^{\beta(E_k - \mu)} + 1}, \quad (34)$$

where  $\beta = (k_B T)^{-1}$ . Therefore, we obtain expressions for 1040 correlation functions (again 1/3 is zero by definition). Their principle structure is equal for Green's functions of the same density class. Table I allows a comparison with the structure of the corresponding inhomogeneities.

density class	inhomogeneity	spectral theorem
IV	$\langle \hat{S} \hat{n}^3 \rangle$	$\langle \hat{S} \hat{n}^4 \rangle$
III	$\langle \hat{S} \hat{n}^2 \rangle$	$\langle \hat{S} \hat{n}^3 \rangle$
II	$\langle \hat{S} \hat{n}^1 \rangle$	$\langle \hat{S} \hat{n}^2 \rangle$
I	$\langle \hat{S} \hat{n}^0 \rangle = \langle \hat{S} \rangle$	$\langle \hat{S} \hat{n}^1 \rangle$

TABLE I: For Green's functions of every density class the principle structure of the correlation functions emerging in the equation of motion (8) and obtained by the spectral theorem (34) is given.

The application of the spectral theorem to Green's functions of density class IV results in correlation functions that do not appear in the spectral weights we are looking for. Only the application to the 960 Green's functions of the remaining density classes is helpful. For each of them the spectral theorem provides an equation that is linear in the correlation functions, because this linearity is given for the spectral weights  $\alpha_k$  in (34). In principle we can therefore write a homogeneous matrix equation for the column of correlation functions  $K_i$ :

$$\begin{pmatrix} a_{1,1} & \dots & a_{1,1040} \\ \vdots & \ddots & \vdots \\ a_{960,1} & \dots & a_{960,1040} \end{pmatrix} \begin{pmatrix} K_1 \\ \vdots \\ \vdots \\ K_{1040} \end{pmatrix} = \begin{pmatrix} 0 \\ \vdots \\ \vdots \\ 0 \end{pmatrix}. \quad (35)$$

Written in this form, equation (35) is underdetermined. This seems to offer the possibility to use additionally the other concept for the correlation functions, that is to make assumptions for certain expectation values or to specify them on the basis of a Hamiltonian that includes lattice effects. To achieve a non-vanishing magnetic order of the system of localized spins it is necessary to specify the spin correlation functions,  $\langle \hat{S} \rangle$ . Lattice effects can be included if these expectation values are based on the Hamiltonian  $\mathcal{H}_{ff} + \mathcal{H}_f$  with

$$\mathcal{H}_f = -b(S_1^z + \eta S_2^z), \quad \eta = \pm 1, \quad (36)$$

as discussed in the forgoing article<sup>4</sup>.

Whenever a certain correlation function is specified, the matrix equation (35) becomes inhomogeneous:

$$\begin{pmatrix} a_{1,1} & \dots & a_{1,x-1} & a_{1,x+1} & \dots \\ \vdots & & \vdots & \vdots & \\ \vdots & & \vdots & \vdots & \\ a_{960,1} & \dots & a_{960,x-1} & a_{960,x+1} & \dots \end{pmatrix} \begin{pmatrix} K_1 \\ \vdots \\ K_{x-1} \\ K_{x+1} \\ \vdots \\ K_{1040} \end{pmatrix} = K_x \begin{pmatrix} a_{1,x} \\ \vdots \\ \vdots \\ a_{960,x} \end{pmatrix}. \quad (37)$$

With the inhomogeneity in the equation of motion of  $\langle \langle c_{i\sigma}; c_{i\sigma}^\dagger \rangle \rangle_E$ , which is 1 by definition, at least one specification is inevitable, enforcing a nontrivial result for the set  $\{K_i\}_i$ .

However, the freedom for the specification of certain correlation functions is drastically reduced because of additional information available. We have already mentioned that 1/3 of the  $K_i$ 's is zero by definition, which reduces the number of unknown variables in (35). Even so, in 1/3 of the cases the application of the spectral theorem (34) does also give zero at the left hand side, this does not lead to a reduction of the number of equations since the right hand side is still a linear relation of the variables. Furthermore, we know that certain pairs of correlation functions have to be identical due to symmetrical reasons.

Hence, we actually do not have an under-determined problem, but rather more equations than variables. The indicator for a proper choice of equations is a nonzero result for the determinant of the matrix in (37). Rules can again best be studied, if the limiting case  $J = 0$ , the Hubbard cluster, is considered.

For an overdetermined problem the introduction of additional specifications for correlation functions is of course problematic. They are likely to contradict some other information we have about the system. For the sake of a connection between cluster and lattice we want to accept that. The consequences shall be demonstrated with an example: If the atomic limit ( $\tilde{T} = 0$ ) is considered, 7 nontrivial correlation functions appear in the spectral weights of the one-particle Green's function. Since the spectral theorem provides only 6 equations,  $\langle S_1^z \rangle$  can be specified on the basis of a Brillouin function for the lattice. However, if a non-vanishing value for  $\langle S_1^z \rangle$  is chosen one has to be aware of the fact that the equality  $\langle S_1^+ c_{1\downarrow}^\dagger c_{1\uparrow} \rangle = \langle S_1^- c_{1\uparrow}^\dagger c_{1\downarrow} \rangle$  will be broken. The equality itself follows from the assumption that expectation values are real, but can also be derived from particle-hole symmetry.

If an equation like (37) needs to be solved exactly for the correlation functions  $\{K_i\}_i$  standard algebraic techniques like Gauss' elimination method can be used. In our work we implemented all these tedious manipulations in a computer program. Its input values are the model parameters and assumed specifications for the correlation functions. By setting successively one and only one

correlation function to 1.0, calculating the set of Green's functions (here the analytical exact expressions are used) and applying the spectral theorem, the matrix (35) is determined. Afterwards the matrix equation (37) is solved numerically exact.

The last step contains a specific numerical problem. Even if a proper set of equations is selected, for large ranges for the chemical potential  $\mu$  the determinant of the matrix in (37) might be rather small. This is connected to the fact that the Fermi distribution function in (34) is almost a step function for low temperatures. The effect can already be studied when looking at the *atomic limit* for the Hubbard model

$$\mathcal{H} = T_0 \sum_{\sigma} \hat{n}_{\sigma} + \frac{U}{2} \sum_{\sigma} \hat{n}_{\sigma} \hat{n}_{-\sigma}. \quad (38)$$

After the application of (34) the two equations ( $\sigma = \uparrow, \downarrow$ )

$$\langle \hat{n}_{\sigma} \rangle = (1 - \langle \hat{n}_{-\sigma} \rangle) f_{-}(T_0) + \langle \hat{n}_{-\sigma} \rangle f_{-}(T_0 + U) \quad (39)$$

define the correlation functions. Whenever  $\mu$  is located well between  $T_0$  and  $T_0 + U$  and additionally  $k_B T \ll U$ , it is  $f_{-}(T_0) - f_{-}(T_0 + U) \approx 1$ . Then (39) becomes

$$\begin{pmatrix} 1 & 1 \\ 1 & 1 \end{pmatrix} \begin{pmatrix} \langle \hat{n}_{\uparrow} \rangle \\ \langle \hat{n}_{\downarrow} \rangle \end{pmatrix} \approx f_{-}(T_0) \begin{pmatrix} 1 \\ 1 \end{pmatrix}, \quad (40)$$

with a vanishing determinant of the matrix. Analytically, one can strictly show that  $\langle \hat{n}_{\uparrow} \rangle = \langle \hat{n}_{\downarrow} \rangle = f_{-}(T_0) [1 + f_{-}(T_0) - f_{-}(T_0 + U)]^{-1}$ . The numerical problem can be avoided if the chemical potential is close to an energy pole or if the temperature is high enough.

For the two-site Hubbard cluster  $\mathcal{H}_s + \mathcal{H}_{ss}$  the mathematical systems are much smaller. Hence, already temperatures around 100 K are sufficient to get meaningful results (see figure 4) over the whole range of the chemical potential (c.p.). In regions for  $\mu$  which are not close to the energy poles all spectral weights remain constant. Figure 4 also nicely illustrates a further consequence of the particle-hole symmetry. As already mentioned above, the energy poles of the one-particle Green's function occur in pairs  $(E_k = T_0 + f_k(\tilde{T}, J, U), \bar{E}_k = T_0 + U - f_k(-\tilde{T}, J, U))$ .

We can now see that for the corresponding spectral weights the implication

$$\alpha_k = \alpha_k(\mu, \sigma, \tilde{T}) \implies \bar{\alpha}_k = \alpha_k(U - \mu, -\sigma, -\tilde{T}), \quad (41)$$

that can be proven analytically, is fulfilled. The signs of  $\tilde{T}$  and  $\sigma$  are not essential because of site and mirror symmetry, respectively. Instead, the  $\mu$ -dependence is the most important feature.

Coming back to the complete CKLM we are again especially interested in the dependence of the cluster properties on  $\tilde{T}$ . For  $\tilde{T} = 0$  we are able to reproduce the *atomic limit* results<sup>3</sup> completely. This includes statements on the spectral weights and the fact that it vanishes for the four additionally emerged energy poles in figure 1. The distribution of the spectral weight for higher

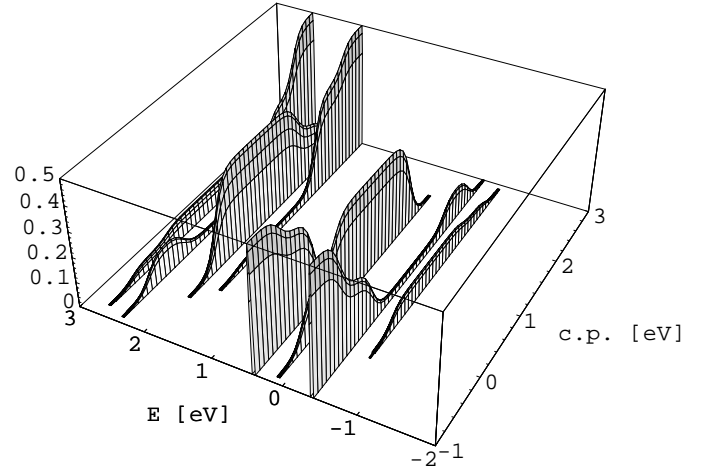


FIG. 4: For the two-site Hubbard-cluster the dependence of the spectral weights of  $\langle\langle c_{i\sigma}; c_{i\sigma}^\dagger \rangle\rangle_E$  on the chemical potential (c.p.) is given. The energy poles are situated at energies  $E$  given in appendix A. The model parameters are:  $T_0 = J = 0$  eV,  $\tilde{T} = 0.4$  eV and  $U = 2$  eV. A temperature of  $T = 100$  K is used.

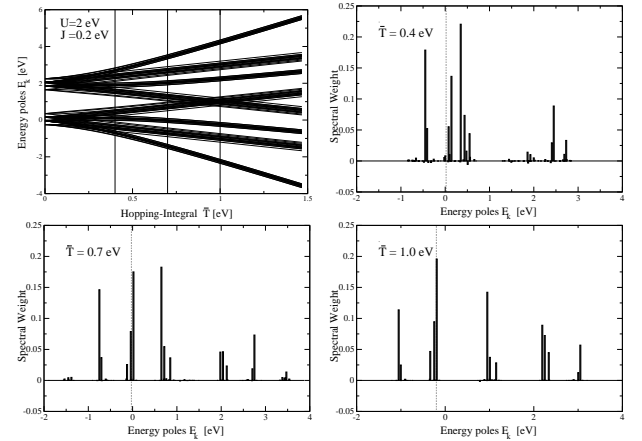


FIG. 5: top left: as figure 2. others: Distribution of the spectral weight of  $\langle\langle c_{i\sigma}; c_{i\sigma}^\dagger \rangle\rangle_E$  for different values of the hopping integral  $\tilde{T}$  (as given). The chemical potential (dotted line) is always chosen such, that the determinant in (37) is not too small. All spin-correlation-functions  $\langle\hat{S}\rangle$  are assumed to be zero. The other model parameters are:  $T_0 = 0.0$  eV,  $J = 0.2$  eV,  $U = 2.0$  eV. Temperature:  $T = 500$  K.

values of  $\tilde{T}$  is shown in figure 5. Especially for  $\tilde{T}$  values higher than 0.5 eV the dominance of the energy poles of the Hubbard cluster can clearly be seen.

The splitting of these poles and a greater width of the bundles in figure 2 is connected to an increase of  $J$ . Nevertheless, a redistribution of spectral weight happens just gradually, as can be seen in figure 6. It is remarkable that up to  $|J| = 0.25$  eV the spectral weight is restricted to a few energy poles. One can also see that some of the energy poles get small negative spectral weights. This is caused by the two problems mentioned above. On the one

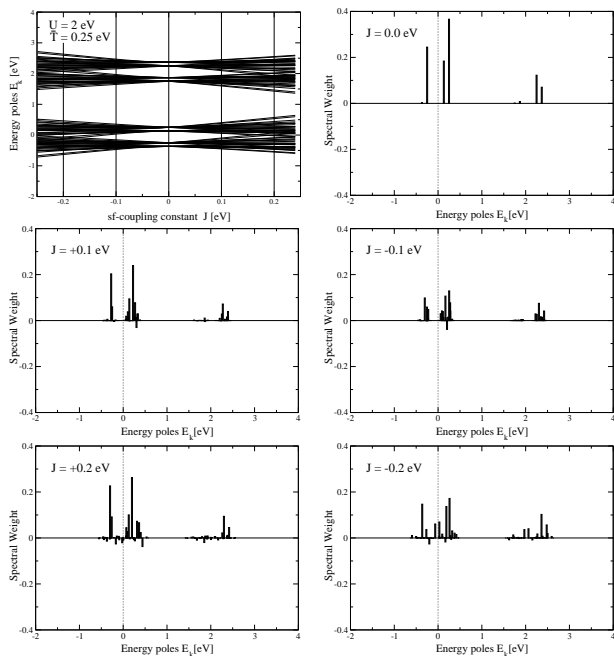


FIG. 6: top left: as figure 3. others: Distribution of the spectral weight of  $\langle\langle c_{i\uparrow}; c_{i\uparrow}^\dagger \rangle\rangle_E$  for different values of the spin-coupling constant  $J$  (as given) with opposite signs. The chemical potential is kept fixed at  $\mu = 0.0$  eV. For the spin expectation values the specification  $\langle S_1^z \rangle = \langle S_2^z \rangle = 0.1$ ;  $\langle S_1^z S_2^z \rangle = \langle S_1^+ S_2^- \rangle = \langle S_1^- S_2^+ \rangle = 0.0$  has been assumed. The other model parameters are:  $T_0 = 0.0$  eV,  $\tilde{T} = 0.25$  eV,  $U = 2.0$  eV. Temperature:  $T = 500$  K.

hand we have specified the values of the spin-correlation functions in figure 6. The choice does certainly not match with calculations based on the two-site Hamiltonian (7). We have stressed above that this might lead to a breakdown of certain symmetries of the cluster. The fact that every spectral weight must be positive, as can be shown with the help of Lehmann's representation, is a property that follows from such symmetries. On the other hand we also mentioned that an unfavourable choice for the chemical potential  $\mu$  implies large numerical errors, due to very small determinants of matrices that need to be inverted. This can also cause negative values for spectral weights.

Our program allows the presentation of the excitation spectrum for various situations. The main intension for the improvement of the *atomic limit* calculations was the ability to treat also an antiferromagnet order of the system of localized spins. An example for typical results is given in figure 7. As in most of the other figures one can see, that even though the Green's function possesses more than 100 energy poles, only a few of them have a non-vanishing spectral weight. The expectation of quasi-continuous energy bands, provoked by pictures for the energy poles as figure 1, is not met by the result obtained from the calculation of the spectral weights. Like in the *atomic limit* we end up with a limited number of

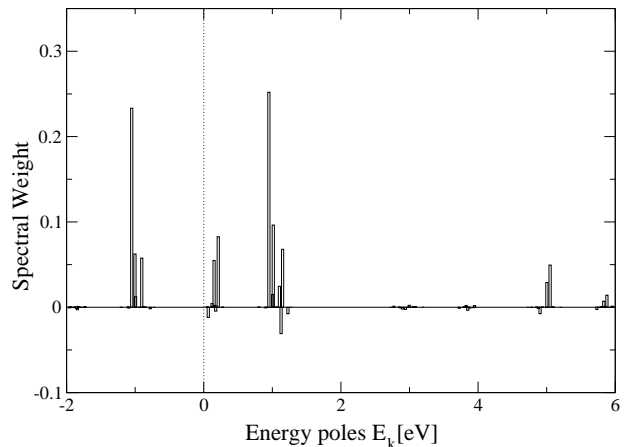


FIG. 7: Distribution of the spectral weight over the energy poles of  $\langle\langle c_{1\uparrow}; c_{1\uparrow}^\dagger \rangle\rangle_E$ . By the specification of the spin-correlation functions  $\langle S_1^z \rangle = 0.1$ ,  $\langle S_2^z \rangle = -0.1$ ;  $\langle S_1^z S_2^z \rangle = \langle S_1^+ S_2^- \rangle = \langle S_1^- S_2^+ \rangle = 0.0$  an antiferromagnetic order is assumed. The model parameters are:  $T_0 = 0.0$  eV,  $\tilde{T} = 1.0$  eV,  $J = 0.2$  eV,  $U = 4.0$  eV. Temperature:  $T = 500$  K.

delta peaks in the spectrum.

#### IV. SUMMARY

We considered the analytical solution for a two-site cluster described by the CKLM. In contrast to a foregoing publication<sup>4</sup> we did not restrict the occupation of the single conduction band. Moreover, a correlation effect in the form of a Hubbard interaction in this band is taken into account. The only remaining constraint is  $S = 1/2$  for the localized spins.

The mathematical effort to achieve the analytical exact result for the Green's function  $\langle\langle c_{i\sigma}; c_{i\sigma}^\dagger \rangle\rangle_E$  is immense. It was the goal of the paper to show that it is still manageable and to explain the necessary techniques. Major points were the separation of the 1040 Green's functions in four density classes, the use of intrinsic symmetries and the study of limiting cases as the empty conduction band and the Hubbard cluster. As a consequence we found the "correct" combinations of Green's functions (appendix B) to obtain system sizes of order  $3 \times 3$ .

The suggested routine for an analytical calculation consists of two main parts. First of all the set of equations of motion needs to be solved by: Combining their inhomogeneities correctly, including the results for higher density classes as in equation (26), inverting the  $3 \times 3$  matrices, performing partial fraction expansions and undoing the combinations of the Green's functions. Secondly, the correlation functions in the spectral weights need to be determined. This happens by: Specifying a desired subset of the correlation functions, applying the spectral theorem to every determined Green's function, selecting



a representative set of these linear equations, using an LU-decomposition to solve the linear system of equations for the unspecified correlation functions.

The first part has been done by hand and the analytical expressions for the obtained 102 energy poles as well as a graphical presentation of the excitation spectrum has been given in this paper. The correlation effect, which leads to a formation of two Hubbard bands, and the characteristic dependence on the important model parameters can clearly be seen in figure 1, 2 and 3. For the second part a computer program has been used, since there exist reliable routines for the numerically exact decomposition of large systems. The resulting vector for the correlation functions was used to discuss the distribution of the spectral weight among the excitation energies. A major conclusion from the provided figures is the concentration of the spectral on a few energy poles. The notion of almost “continuous” bands formed by 102 energies is not confirmed if the numerators of the Green’s functions are considered.

We propose to use a subset of the correlation functions in the numerators of the Green’s functions to construct a connection of the cluster to the lattice. This freedom in

the specification of expectation values strongly influences the results for the spectral weights. We have pointed out, that as a possible side effect of this procedure symmetries of the cluster might be destroyed, leading to certain unphysical features.

We intend to use the results of this work as a limiting case to test various approximations for the complete CKLM. Furthermore, the cluster result itself can serve as a starting point for an approximation of the lattice. We are convinced that techniques similar to what has been proposed here can be used to treat slightly more complex systems, like a cluster with a higher value for the localized spin  $S$  or another number of lattice sites.

### Acknowledgments

One of us (T. H.) gratefully acknowledges the financial support of the *Studienstiftung des deutschen Volkes*. This work also benefitted from the financial support of the *Sonderforschungsbereich SFB 290* of the Deutsche Forschungsgemeinschaft.

## APPENDIX A: THE HUBBARD CLUSTER

An analytical solution of a two-site Hubbard cluster has already been given by several authors<sup>6,7,8</sup>. We present here a direct solution, that is compatible to the language of equations of motion used in the rest of the paper.

We study the Hamiltonian

$$\mathcal{H} = \sum_{\sigma} \left\{ \tilde{T} \left( c_{1\sigma}^{\dagger} c_{2\sigma} + c_{2\sigma}^{\dagger} c_{1\sigma} \right) + \frac{U}{2} \sum_{k=1}^2 \hat{n}_{k\sigma} \hat{n}_{k-\sigma} \right\}. \quad (\text{A1})$$

Using abbreviation (9) we need to consider a set of Green’s functions which is almost identical to the list given in section II. However, in contrast to the CKLM cluster we have  $\hat{S} \equiv 1$  what decreases the number of functions drastically. We are left with the following set of equations of motion, written again in a matrix representation:

$$E \begin{pmatrix} G_A \\ G_B \\ G_C \\ G_D \\ G_F \\ G_G \\ G_H \\ G_J \\ G_K \\ G_L \\ G_M \end{pmatrix} - \begin{pmatrix} \epsilon\tilde{T} & U & & & & & & & & & \\ & U & \epsilon\tilde{T} & \epsilon\tilde{T} & -\epsilon\tilde{T} & & & & & & \\ & \epsilon\tilde{T} & & -\epsilon\tilde{T} & \epsilon\tilde{T} & U & & & & & \\ & \epsilon\tilde{T} & -\epsilon\tilde{T} & & \epsilon\tilde{T} & & U & & & & \\ & -\epsilon\tilde{T} & \epsilon\tilde{T} & \epsilon\tilde{T} & U & & -U & & & & \\ & & & & & \epsilon\tilde{T} + U & & & & & \\ & & & & & & & U & \epsilon\tilde{T} & -\epsilon\tilde{T} & \\ & & & & & & \epsilon\tilde{T} & & -\epsilon\tilde{T} & \epsilon\tilde{T} & \\ & & & & & & \epsilon\tilde{T} & -\epsilon\tilde{T} & U & \epsilon\tilde{T} & \\ & & & & & & -\epsilon\tilde{T} & \epsilon\tilde{T} & \epsilon\tilde{T} & & U \\ & & & & & & & & & \epsilon\tilde{T} + U & \end{pmatrix} \begin{pmatrix} G_A \\ G_B \\ G_C \\ G_D \\ G_F \\ G_G \\ G_H \\ G_J \\ G_K \\ G_L \\ G_M \end{pmatrix} = \begin{pmatrix} K_A \\ K_B \\ K_C \\ K_D \\ K_F \\ K_G \\ K_H \\ K_J \\ K_K \\ K_L \\ K_M \end{pmatrix} \quad (\text{A2})$$

It is now essential to introduce the combinations

$$\begin{aligned}
X_b^{(\epsilon)} &= X_B^{(\epsilon)} + X_F^{(\epsilon)}, & X_f^{(\epsilon)} &= X_B^{(\epsilon)} - X_F^{(\epsilon)}, \\
X_c^{(\epsilon)} &= X_C^{(\epsilon)} + X_D^{(\epsilon)}, & X_d^{(\epsilon)} &= X_C^{(\epsilon)} - X_D^{(\epsilon)}, \\
X_k^{(\epsilon)} &= X_K^{(\epsilon)} + X_H^{(\epsilon)}, & X_h^{(\epsilon)} &= X_K^{(\epsilon)} - X_H^{(\epsilon)}, \\
X_l^{(\epsilon)} &= X_L^{(\epsilon)} + X_J^{(\epsilon)}, & X_j^{(\epsilon)} &= X_L^{(\epsilon)} - X_J^{(\epsilon)},
\end{aligned} \tag{A3}$$

where “ $X$ ” stands for “ $G$ ” or “ $K$ ”. As one can see the matrix representation of the original equations of motion contains blocks of the size  $4 \times 4$ . After the proposed combination the remaining maximum block size is  $2 \times 2$ , which can easily be inverted:

$$\begin{pmatrix} \hat{E} - U & -2\tilde{T} \\ -2\tilde{T} & \hat{E} \end{pmatrix}^{-1} = \sum_{\gamma=\pm 1} \frac{\frac{1}{2} \begin{pmatrix} 1 & 0 \\ 0 & 1 \end{pmatrix} + \gamma \frac{1}{4b} \begin{pmatrix} U & 4\tilde{T} \\ 4\tilde{T} & -U \end{pmatrix}}{\hat{E} - \frac{U}{2} - \gamma b} \tag{A4}$$

The form of the energy constant  $b = \sqrt{\left(\frac{U}{2}\right)^2 + 4\tilde{T}^2}$  demonstrates, that quadratic system sizes are inevitable. We get the following matrix for the equations of motion:

$$E \begin{pmatrix} G_A \\ G_b \\ G_c \\ G_f \\ G_d \\ G_G \\ G_h \\ G_j \\ G_k \\ G_l \\ G_M \end{pmatrix} - \begin{pmatrix} \epsilon\tilde{T} & \frac{U}{2} & \frac{U}{2} & & & & & & & & \\ & U - \epsilon\tilde{T} & 2\epsilon\tilde{T} & & & & & & & & \\ & 2\epsilon\tilde{T} & -\epsilon\tilde{T} & & & & & & & & \\ & & & U + \epsilon\tilde{T} & & & & & & & \\ & & & \epsilon\tilde{T} & U & & & & & & \\ & & & & \epsilon\tilde{T} + U & & & & & & \\ & & & & & U - \epsilon\tilde{T} & 2\epsilon\tilde{T} & & & & \\ & & & & & 2\epsilon\tilde{T} & -\epsilon\tilde{T} & & & & \\ & & & & & & & U + \epsilon\tilde{T} & & & \\ & & & & & & & \epsilon\tilde{T} & U & & \\ & & & & & & & & \epsilon\tilde{T} + U & & \end{pmatrix} \begin{pmatrix} G_A \\ G_b \\ G_c \\ G_f \\ G_d \\ G_G \\ G_h \\ G_j \\ G_k \\ G_l \\ G_M \end{pmatrix} = \begin{pmatrix} K_A \\ K_b \\ K_c \\ K_f \\ K_d \\ K_G \\ K_h \\ K_j \\ K_k \\ K_l \\ K_M \end{pmatrix} \tag{A5}$$

What remains is a straightforward solution of (A5). The expression of  $G_M^{(\epsilon)}$  can immediately be written down. To get  $G_l^{(\epsilon)}$  and  $G_k^{(\epsilon)}$  in a form with linear energy poles, a single partial fraction expansion is necessary. For  $G_h^{(\epsilon)}$  and  $G_j^{(\epsilon)}$  one has to apply (A4). And with a few more steps one gets

$$\begin{aligned}
G_A^{(\epsilon)} &= \frac{K_A}{E - \epsilon\tilde{T}} - \frac{K_b^{(\epsilon)} + K_c^{(\epsilon)} + K_f^{(\epsilon)}}{2(E - \epsilon\tilde{T})} + \frac{K_S^{(\epsilon)}}{2(E - \epsilon\tilde{T})} + \frac{K_f^{(\epsilon)} + K_S^{(\epsilon)}}{2(E - \epsilon\tilde{T} - U)} \\
&+ \sum_{\gamma=\pm 1} \left\{ \frac{\left(1 + \gamma \frac{2\epsilon\tilde{T}}{b} + \gamma \frac{U}{2b}\right) K_b^{(\epsilon)} + \left(1 + \gamma \frac{2\epsilon\tilde{T}}{b} - \gamma \frac{U}{2b}\right) K_c^{(\epsilon)}}{4(E + \epsilon\tilde{T} - \frac{U}{2} - \gamma b)} - \frac{\left(1 + \gamma \frac{2\epsilon\tilde{T}}{b}\right) K_S^{(\epsilon)}}{2(E + \epsilon\tilde{T} - \frac{U}{2} - \gamma b)} \right\}.
\end{aligned} \tag{A6}$$

We have defined the sum of correlation functions

$$K_S^{(\epsilon)} = \epsilon \langle \hat{n}_{\bar{s}\sigma} c_{\bar{s}-\sigma}^\dagger c_{s-\sigma} \rangle - \langle c_{s-\sigma}^\dagger c_{\bar{s}-\sigma} c_{s\sigma}^\dagger c_{\bar{s}\sigma} \rangle + \epsilon \langle \hat{n}_{\bar{s}\sigma} c_{s-\sigma}^\dagger c_{\bar{s}-\sigma} \rangle - \langle c_{\bar{s}-\sigma}^\dagger c_{s-\sigma} c_{s\sigma}^\dagger c_{\bar{s}\sigma} \rangle + \langle \hat{n}_{\bar{s}-\sigma} \hat{n}_{s-\sigma} \rangle. \tag{A7}$$

As a last step on the way to the desired single-particle Green's function one has to undo the combination (9) by considering the sum  $\frac{1}{2} (G_A^{(+)} + G_A^{(-)})$ . Then we obtain the result

$$\begin{aligned}
\langle\langle c_{s\sigma}; c_{s\sigma}^\dagger \rangle\rangle_E &= \frac{2 - K_b^{(+)} - K_c^{(+)} - K_f^{(+)} + K_S^{(+)}}{4(E - \tilde{T})} + \frac{K_f^{(+)} + K_S^{(+)}}{4(E - \tilde{T} - U)} \\
&+ \frac{2 - K_b^{(-)} - K_c^{(-)} - K_f^{(-)} + K_S^{(-)}}{4(E + \tilde{T})} + \frac{K_f^{(-)} + K_S^{(-)}}{4(E + \tilde{T} - U)}
\end{aligned}$$

$$\begin{aligned}
& + \frac{\left(1 + \frac{2\tilde{T}}{b}\right) (K_b^{(+)} + K_c^{(+)} - 2K_S^{(+)}) + \frac{U}{2b}(K_b^{(+)} - K_c^{(+)})}{8(E + \tilde{T} - \frac{U}{2} - b)} \\
& + \frac{\left(1 - \frac{2\tilde{T}}{b}\right) (K_b^{(+)} + K_c^{(+)} - 2K_S^{(+)}) - \frac{U}{2b}(K_b^{(+)} - K_c^{(+)})}{8(E + \tilde{T} - \frac{U}{2} + b)} \\
& + \frac{\left(1 - \frac{2\tilde{T}}{b}\right) (K_b^{(-)} + K_c^{(-)} - 2K_S^{(-)}) + \frac{U}{2b}(K_b^{(-)} - K_c^{(-)})}{8(E - \tilde{T} - \frac{U}{2} - b)} \\
& + \frac{\left(1 + \frac{2\tilde{T}}{b}\right) (K_b^{(-)} + K_c^{(-)} - 2K_S^{(-)}) - \frac{U}{2b}(K_b^{(-)} - K_c^{(-)})}{8(E - \tilde{T} - \frac{U}{2} + b)}.
\end{aligned}$$

## APPENDIX B: COMBINATIONS OF GREEN'S FUNCTIONS

First of all the notation for the Green's functions needs to be clarified. Each of them gets to subindex that consists of a number and a letter. The latter part has already been introduced above when the list of Green's functions with different possibilities for the fermionic operators is given. The former part enumerates the possibilities for spin operators  $\hat{S}$ . The numbers  $1, \dots, 10$  are used for  $\hat{S} = 1, S_s^z, S_s^z, S_s^{-\sigma}, S_s^{-\sigma}, S_s^z S_s^z, S_s^z S_s^{-\sigma}, S_s^z S_s^{-\sigma}, S_s^{-\sigma} S_s^z, S_s^{-\sigma} S_s^z$ . Additionally, the Green's functions  $\langle\langle \hat{S} c_{s-\sigma}^\dagger c_{s\sigma} c_{s\sigma} \rangle\rangle_{Nx}^{(\epsilon)}$ , and  $\langle\langle \hat{S} \hat{n}_{s\sigma} c_{s\sigma}^\dagger c_{s-\sigma} c_{s-\sigma} \rangle\rangle_{Px}^{(\epsilon)}$  with  $x = 1, \dots, 5$  for  $\hat{S} = S_s^\sigma, S_s^\sigma, S_s^z S_s^\sigma, S_s^z S_s^\sigma, S_s^{-\sigma} S_s^{-\sigma}$  appear in the necessary equations of motion. Each Green's function taken 8 times for the different possibilities for  $s, \sigma$  and  $\epsilon$  gives the number 1040.

The first step of combinations is determined by the spin operators. We use the rules that have been applied to the insulator<sup>4</sup>.

$$\begin{aligned}
H_{2\dots}^{(\pm)} &= \frac{\hbar^2}{4} G_{1\dots} \pm \frac{\hbar}{2} G_{2\dots} \pm \frac{\hbar}{2} G_{3\dots} + G_{6\dots} \\
H_{3\dots}^{(\pm)} &= \frac{\hbar^2}{4} G_{1\dots} \mp \frac{\hbar}{2} G_{2\dots} \pm \frac{\hbar}{2} G_{3\dots} - G_{6\dots} \\
H_{4\dots}^{(\pm)} &= \frac{\hbar}{2} G_{4\dots} \pm G_{7\dots} \\
H_{5\dots}^{(\pm)} &= \frac{\hbar}{2} G_{5\dots} \pm G_{8\dots} \\
H_{N1}^{(\pm)} &= \frac{\hbar}{2} G_{N1} \pm G_{N3} & H_{P1}^{(\pm)} &= \frac{\hbar}{2} G_{P1} \pm G_{P3} \\
H_{N2}^{(\pm)} &= \frac{\hbar}{2} G_{N2} \pm G_{N4} & H_{P2}^{(\pm)} &= \frac{\hbar}{2} G_{P2} \pm G_{P4}
\end{aligned}$$

The next step produces the correct combinations of fermionic operators of different Green's functions. We use the rules (A3) applied to the Hubbard cluster.

### Density class III

$$\begin{aligned}
H_{4l}^{(-)} &= H_{4L}^{(-)} + H_{5J}^{(-)} & H_{5l}^{(-)} &= H_{5L}^{(-)} + H_{4J}^{(-)} & H_{2l}^{(\pm)} &= H_{2L}^{(\pm)} + H_{2J}^{(\pm)} \\
H_{4k}^{(-)} &= H_{4K}^{(-)} + H_{5H}^{(-)} & H_{5k}^{(-)} &= H_{5K}^{(-)} + H_{4H}^{(-)} & H_{2k}^{(\pm)} &= H_{2K}^{(\pm)} + H_{2H}^{(\pm)} \\
H_{5h}^{(-)} &= H_{4K}^{(-)} - H_{5H}^{(-)} & H_{4h}^{(-)} &= H_{5K}^{(-)} - H_{4H}^{(-)} & H_{2h}^{(\pm)} &= H_{2K}^{(\pm)} - H_{2H}^{(\pm)} \\
H_{5j}^{(-)} &= H_{4L}^{(-)} - H_{5J}^{(-)} & H_{4j}^{(-)} &= H_{5L}^{(-)} - H_{4J}^{(-)} & H_{2j}^{(\pm)} &= H_{2L}^{(\pm)} - H_{2J}^{(\pm)} \\
\\ 
H_{3g}^{(-)} &= H_{3G}^{(-)} + G_{10G} & H_{4g}^{(+)} &= H_{4G}^{(+)} + H_{5G}^{(+)} & H_{p1}^{(-)} &= H_{P1}^{(-)} + H_{P2}^{(-)} \\
H_{3g}^{(+)} &= H_{3G}^{(+)} + G_{9G} & H_{5g}^{(+)} &= H_{4G}^{(+)} - H_{5G}^{(+)} & H_{p2}^{(-)} &= H_{P1}^{(-)} - H_{P2}^{(-)} \\
H_{6g}^{(-)} &= H_{3G}^{(-)} - G_{10G} & H_{4g}^{(*)} &= H_{4G}^{(-)} + H_{P2}^{(+)} & H_{p2}^{(*)} &= H_{4G}^{(-)} - H_{P2}^{(+)} \\
H_{6g}^{(+)} &= H_{3G}^{(+)} - G_{9G} & H_{5g}^{(*)} &= H_{5G}^{(-)} + H_{P1}^{(+)} & H_{p1}^{(*)} &= H_{5G}^{(-)} - H_{P1}^{(+)} \\
& & H_{2g}^{(+)} &= H_{2G}^{(+)} + G_{P5} & H_{p5}^{(+)} &= H_{2G}^{(+)} - G_{P5}
\end{aligned}$$

$$\begin{aligned}
H_{4j+5j}^{(++)} &= (H_{4L}^{(+)} - H_{4J}^{(+)} + (H_{5L}^{(+)} - H_{5J}^{(+)})) \\
H_{4h+5h}^{(++)} &= (H_{4K}^{(+)} - H_{4H}^{(+)} + (H_{5K}^{(+)} - H_{5H}^{(+)})) \\
H_{4h-5h}^{(++)} &= (H_{4K}^{(+)} - H_{4H}^{(+)} - (H_{5K}^{(+)} - H_{5H}^{(+)})) \\
H_{6l-6j}^{(-+)} &= (H_{3J}^{(-)} - G_{9L}) - (H_{3L}^{(+)} - G_{10J}) \\
H_{6h+6k}^{(-+)} &= (H_{3K}^{(-)} - G_{9H}) + (H_{3H}^{(+)} - G_{10K}) \\
H_{6h-6k}^{(-+)} &= (H_{3K}^{(-)} - G_{9H}) - (H_{3H}^{(+)} - G_{10K}) \\
H_{6k+6h}^{(-+)} &= (H_{3H}^{(-)} - G_{9K}) + (H_{3K}^{(+)} - G_{10H}) \\
H_{6k-6h}^{(-+)} &= (H_{3H}^{(-)} - G_{9K}) - (H_{3K}^{(+)} - G_{10H}) \\
H_{6j-6l}^{(-+)} &= (H_{3L}^{(-)} - G_{9J}) - (H_{3J}^{(+)} - G_{10L}) \\
H_{4j-5j}^{(++)} &= (H_{4L}^{(+)} - H_{4J}^{(+)} - (H_{5L}^{(+)} - H_{5J}^{(+)})) \\
H_{6l+6j}^{(-+)} &= (H_{3J}^{(-)} - G_{9L}) + (H_{3L}^{(+)} - G_{10J}) \\
H_{6j+6l}^{(-+)} &= (H_{3L}^{(-)} - G_{9J}) + (H_{3J}^{(+)} - G_{10L}) \\
H_{4k+5k}^{(++)} &= (H_{4K}^{(+)} + H_{4H}^{(+)} + (H_{5K}^{(+)} + H_{5H}^{(+)})) \\
H_{4k-5k}^{(++)} &= (H_{4K}^{(+)} + H_{4H}^{(+)} - (H_{5K}^{(+)} + H_{5H}^{(+)})) \\
H_{4l-5l}^{(++)} &= (H_{4L}^{(+)} + H_{4J}^{(+)} - (H_{5L}^{(+)} + H_{5J}^{(+)})) \\
H_{3j-3l}^{(-+)} &= (H_{3J}^{(-)} + G_{9L}) - (H_{3L}^{(+)} + G_{10J}) \\
H_{3h+3k}^{(-+)} &= (H_{3H}^{(-)} + G_{9K}) + (H_{3K}^{(+)} + G_{10H}) \\
H_{3h-3k}^{(-+)} &= (H_{3H}^{(-)} + G_{9K}) - (H_{3K}^{(+)} + G_{10H}) \\
H_{3k+3h}^{(-+)} &= (H_{3K}^{(-)} + G_{9H}) + (H_{3H}^{(+)} + G_{10K}) \\
H_{3k-3h}^{(-+)} &= (H_{3K}^{(-)} + G_{9H}) - (H_{3H}^{(+)} + G_{10K}) \\
H_{3l-3j}^{(-+)} &= (H_{3L}^{(-)} + G_{9J}) - (H_{3J}^{(+)} + G_{10L}) \\
H_{4l+5l}^{(++)} &= (H_{4L}^{(+)} + H_{4J}^{(+)} + (H_{5L}^{(+)} + H_{5J}^{(+)})) \\
H_{3j+3l}^{(-+)} &= (H_{3J}^{(-)} + G_{9L}) + (H_{3L}^{(+)} + G_{10J}) \\
H_{3l+3j}^{(-+)} &= (H_{3L}^{(-)} + G_{9J}) + (H_{3J}^{(+)} + G_{10L})
\end{aligned}$$

### Density class II

$$\begin{aligned}
H_{4b}^{(+)} &= H_{4B}^{(+)} + H_{5F}^{(+)} & H_{5b}^{(+)} &= H_{5B}^{(+)} + H_{4F}^{(+)} & H_{2b}^{(\pm)} &= H_{2B}^{(\pm)} + H_{2F}^{(\pm)} \\
H_{4c}^{(+)} &= H_{4C}^{(+)} + H_{5D}^{(+)} & H_{5c}^{(+)} &= H_{5C}^{(+)} + H_{4D}^{(+)} & H_{2c}^{(\pm)} &= H_{2C}^{(\pm)} + H_{2D}^{(\pm)} \\
H_{5d}^{(+)} &= H_{4C}^{(+)} - H_{5D}^{(+)} & H_{4d}^{(+)} &= H_{5C}^{(+)} - H_{4D}^{(+)} & H_{2d}^{(\pm)} &= H_{2C}^{(\pm)} - H_{2D}^{(\pm)} \\
H_{5f}^{(+)} &= H_{4B}^{(+)} - H_{5F}^{(+)} & H_{4f}^{(+)} &= H_{5B}^{(+)} - H_{4F}^{(+)} & H_{2f}^{(\pm)} &= H_{2B}^{(\pm)} - H_{2F}^{(\pm)} \\
H_{3r}^{(+)} &= H_{3R}^{(+)} + G_{10R} & H_{4r}^{(-)} &= H_{4R}^{(-)} + H_{5R}^{(-)} & H_{n1}^{(+)} &= H_{N1}^{(+)} + H_{N2}^{(+)} \\
H_{3r}^{(-)} &= H_{3R}^{(-)} + G_{9R} & H_{5r}^{(-)} &= H_{4R}^{(-)} - H_{5R}^{(-)} & H_{n2}^{(+)} &= H_{N1}^{(+)} - H_{N2}^{(+)} \\
H_{6r}^{(+)} &= H_{3R}^{(+)} - G_{10R} & H_{4r}^{(*)} &= H_{4R}^{(+)} + H_{N2}^{(-)} & H_{n2}^{(*)} &= H_{4R}^{(+)} - H_{N2}^{(-)} \\
H_{6r}^{(-)} &= H_{3R}^{(-)} - G_{9R} & H_{5r}^{(*)} &= H_{5R}^{(+)} + H_{N1}^{(-)} & H_{n1}^{(*)} &= H_{5R}^{(+)} - H_{N1}^{(-)} \\
H_{2r}^{(-)} &= H_{2R}^{(-)} + G_{N5} & H_{n5}^{(-)} &= H_{2R}^{(-)} - G_{N5} \\
H_{4b+5b}^{(---)} &= (H_{4B}^{(-)} + H_{4F}^{(-)} + (H_{5B}^{(-)} + H_{5F}^{(-)})) & H_{4d+5d}^{(---)} &= (H_{4C}^{(-)} - H_{4D}^{(-)} + (H_{5C}^{(-)} - H_{5D}^{(-)})) \\
H_{4c+5c}^{(---)} &= (H_{4C}^{(-)} + H_{4D}^{(-)} + (H_{5C}^{(-)} + H_{5D}^{(-)})) & H_{4d-5d}^{(---)} &= (H_{4C}^{(-)} - H_{4D}^{(-)} - (H_{5C}^{(-)} - H_{5D}^{(-)})) \\
H_{4c-5c}^{(---)} &= (H_{4C}^{(-)} + H_{4D}^{(-)} - (H_{5C}^{(-)} + H_{5D}^{(-)})) & H_{4f-5f}^{(---)} &= (H_{4B}^{(-)} - H_{4F}^{(-)} - (H_{5B}^{(-)} - H_{5F}^{(-)})) \\
H_{3b+3f}^{(+-)} &= (H_{3B}^{(+)} + G_{9F}) + (H_{3F}^{(-)} + G_{10B}) & H_{6b+6f}^{(+-)} &= (H_{3F}^{(+)} - G_{9B}) + (H_{3B}^{(-)} - G_{10F}) \\
H_{3c+3d}^{(+-)} &= (H_{3C}^{(+)} + G_{9D}) + (H_{3D}^{(-)} + G_{10C}) & H_{6c+6d}^{(+-)} &= (H_{3D}^{(+)} - G_{9C}) + (H_{3C}^{(-)} - G_{10D}) \\
H_{3c-3d}^{(+-)} &= (H_{3C}^{(+)} + G_{9D}) - (H_{3D}^{(-)} + G_{10C}) & H_{6c-6d}^{(+-)} &= (H_{3D}^{(+)} - G_{9C}) - (H_{3C}^{(-)} - G_{10D}) \\
H_{3c+3d}^{(-+)} &= (H_{3C}^{(-)} + G_{10D}) + (H_{3D}^{(+)} + G_{9C}) & H_{6c+6d}^{(-+)} &= (H_{3D}^{(-)} - G_{10C}) + (H_{3C}^{(+)} - G_{9D}) \\
H_{3c-3d}^{(-+)} &= (H_{3C}^{(-)} + G_{10D}) - (H_{3D}^{(+)} + G_{9C}) & H_{6c-6d}^{(-+)} &= (H_{3D}^{(-)} - G_{10C}) - (H_{3C}^{(+)} - G_{9D}) \\
H_{3b+3f}^{(-+)} &= (H_{3B}^{(-)} + G_{10F}) + (H_{3F}^{(+)} + G_{9B}) & H_{6b+6f}^{(-+)} &= (H_{3F}^{(-)} - G_{10B}) + (H_{3B}^{(+)} - G_{9F}) \\
H_{4b-5b}^{(---)} &= (H_{4B}^{(-)} + H_{4F}^{(-)} - (H_{5B}^{(-)} + H_{5F}^{(-)})) & H_{4f+5f}^{(---)} &= (H_{4B}^{(-)} - H_{4F}^{(-)} + (H_{5B}^{(-)} - H_{5F}^{(-)})) \\
H_{3b-3f}^{(-+)} &= (H_{3B}^{(-)} + G_{10F}) - (H_{3F}^{(+)} + G_{9B}) & H_{6b-6f}^{(-+)} &= (H_{3F}^{(+)} - G_{9B}) - (H_{3B}^{(-)} - G_{10F}) \\
H_{3b-3f}^{(+-)} &= (H_{3B}^{(+)} + G_{9F}) - (H_{3F}^{(-)} + G_{10B}) & H_{6b-6f}^{(+-)} &= (H_{3F}^{(-)} - G_{10B}) - (H_{3B}^{(+)} - G_{9F})
\end{aligned}$$

---

\* Electronic address: hickel@physik.hu-berlin.de

<sup>1</sup> C. Zener, Phys. Rev. **81**, 440 (1951).

<sup>2</sup> see for instance: S. Ishihara, J. Inoue and S. Maekawa, Phys. Rev. B **55**, 8280 (1997). Y. Imai and N. Kawakami, J. Phys. Soc. Jpn. **69**, 3063 (2000). K. Held and D. Vollhardt, Phys. Rev. Lett. **84**, 5168 (2000).

<sup>3</sup> W. Nolting and M. Matlak, phys. stat. sol. (b) **123**, 155 (1984).

<sup>4</sup> T. Hickel, J. Röseler and W. Nolting, cond-mat/0211655.

<sup>5</sup> T. Hickel *Exact Statements on the correlated Kondo-Lattice Model* (diploma thesis, Department of Physics, Humboldt-Universität zu Berlin, 2001).

<sup>6</sup> R. Schumann, cond-mat/0101476 (2001).

<sup>7</sup> A. Avella, F. Mancini, T. Saikawa, cond-mat/0103610 (2001).

<sup>8</sup> M. Matlak, 1999 (private communication).